2024 IEEE/RSJ International Conference on Intelligent Robots and Systems (IROS)
October 14-18, 2024. Abu Dhabi, UAE

# Energy Minimization using Custom-Designed Magnetic-Spring Actuators

Yue Yang Fu, Ali U. Kilic, and David J. Braun

***Abstract*— This study introduces an innovative actuator that resembles a motor with a non-uniform permanent magnetic field. We have developed a prototype of the actuator by combining a standard motor, characterized by a uniform magnetic field, with a custom rotary magnetic spring exhibiting a non-uniform magnetic field. We have also presented a systematic computational approach to customize the magnetic field to minimize the energy consumption of the actuator when used for a user-defined oscillatory task. Experiments demonstrate that this optimized actuator significantly lowers energy consumption in a typical oscillatory task, such as pick-and-place or oscillatory limb motion during locomotion, compared to conventional motors. Our findings imply that incorporating task-optimized non-uniform permanent magnetic fields into conventional motors and direct-drive actuators could enhance the energy efficiency of robotic systems.**

## I. Introduction

The rising adoption of robots in industrial settings has motivated research into innovative methods for reducing energy consumption. In the context of robotic motions, motors are energetically active elements that provide torque for actuation. However, motors also require energy to generate torque even when not performing mechanical work. In contrast, springs are energetically passive components that can provide torque without requiring external energy. Therefore, combining a spring in parallel with a motor can reduce the energy consumption of a motor when performing both static weight-bearing [1] and dynamic oscillatory tasks [2]–[4]. In a typical oscillatory task, the spring can provide almost all the required torque, while the motor only needs to overcome friction and suppress disturbances faster than the spring alone could. This approach makes it appealing to improve the energy efficiency of robots by using parallel elastic actuators that combine motors with springs.

The energy efficiency of parallel elastic actuators when performing static weight-bearing or dynamic oscillatory tasks has been highlighted in several studies. Common examples include energetically passive gravity compensation mechanisms [5], simple devices used to augment human motion [6], robot exoskeletons [7], [8], and actuators [9], [10] designed for repetitive tasks. In all these applications, effectively reducing the energy cost requires optimization of the torque-deflection behavior of the spring. Most parallel elastic actuators are designed using mechanical springs, although other types of springs such as magnetic springs [11] could be used. In addition to producing unique torque-displacement curves [12], magnetic springs are not subject to fatigue and failure like their mechanical counterparts [13], and may be easier to customize, as they can be built by leveraging established technology used to design permanent magnet motors. In general, actuators with customized torque-deflection behavior may play a crucial role in achieving energy-efficient motion, somewhat similar to biological systems [14].

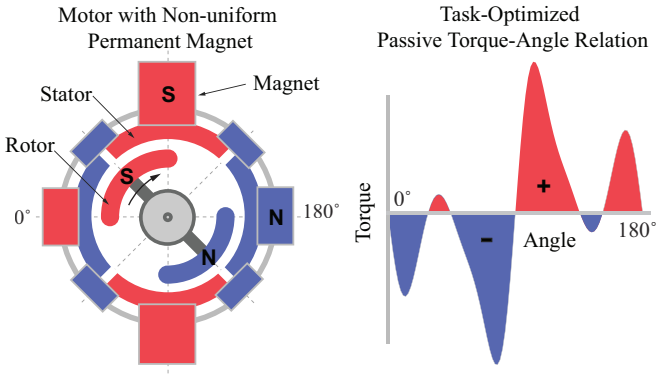


Fig. 1. Left: Conceptual model of the rotary magnetic spring actuator that has a non-uniform permanent magnetic field. Right: Task-optimized passive torque-angle characteristic of the actuator.

In this paper, we present a non-uniform permanent magnetic field actuator implemented by connecting a motor in parallel with a rotary magnet spring. Most models of rotary magnetic springs are created by arranging permanent magnets in coaxial rings [15] and cylinders [16], or by stacking annular magnets together [17]. Whereas these previous works elaborate novel designs for magnetic springs, we introduce the concept of customizable rotary magnet springs – implemented here using small disk-shaped permanent magnets stacked around a cylindrical stator – to achieve a user-defined oscillatory trajectory with significantly lower torque compared to a motor. Consistent with our theoretical predictions, experimental results demonstrate a significant reduction in the maximal torque and the energy consumption of the actuator compared to a conventional motor when both are used to realize the same user-defined oscillatory task.

The paper is organized as follows. In Section II, we use a simple case study example to explore the benefit of an optimally designed motor-spring actuator compared to a motor alone. In Section III, we present the optimization

Yue Yang Fu is affiliated with the Department of Electrical and Computer Engineering and the SyBBURE Searle Undergraduate Research Program at Vanderbilt University and was a student researcher with the Advanced Robotics and Control Laboratory at the time this work was conducted. Ali U. Kilic and David J. Braun were affiliated with the Advanced Robotics and Control Laboratory at Vanderbilt University during this work. This research was supported by the National Science Foundation through the CAREER Award under Grant No. NSF 2144551.

method that can be used to systematically design rotary magnetic springs for motor-spring actuators. In Section IV, we present the prototype of a motor-spring actuator and report experimental results demonstrating the benefit of the optimally designed actuator compared to a motor.

## II. Energy Minimization using a Simple Motor-Spring Actuator

In this section, we explore the advantage of using a magnetic spring in parallel with the motor for an oscillatory task in a simple case study example. Our results show that the spring can be used to provide most of the torque required to perform an oscillatory task leading to substantial energy saving as opposed to using the motor alone.

### A. Model

To explore the benefit of a rotary magnetic spring, we consider an inertial load representing the robot, attached to a motor and a magnetic spring as shown in Fig. 2.

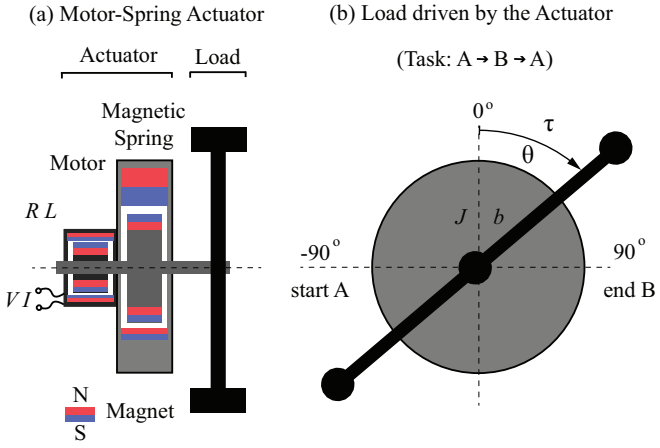


Fig. 2. Model of the Motor-Spring Actuator attached to an inertial load.

The equation of motion for the actuator and the load is given by

$$J\ddot{\theta} + b\dot{\theta} = \tau, \tag{1}$$

where $J$ is the moment of inertia of the actuator and the load, $b$ is the damping coefficient, and $\tau$ is the torque of the actuator.

The torque of the actuator is composed of the torque of the motor and the torque produced by the magnetic spring,

$$\tau = \tau_m + \tau_s. \tag{2}$$

The torque of the magnetic spring depends on the design of the magnetic spring. For simplicity, here we assume that the magnetic spring acts like a linear spring,

$$\tau_s = -k_s\theta, \tag{3}$$

where $k_s$ is the stiffness of the magnetic spring.

The torque of the motor is given by

$$\tau_m = k_m I, \tag{4}$$

where $k_m$ is the motor torque constant while $I$ is the motor current, defined by the electrical side motor dynamics

$$L\dot{I} + RI + k_b\dot{\theta} = V, \tag{5}$$

where $V$ is the input voltage to the motor, $R$ is the internal resistance of the motor, and $k_b$ is the back-emf constant.

In the next section, we explore the benefit of the magnetic spring in reducing the motor torque when performing an oscillatory task.

### B. Task

A pick-and-place task refers to a common operation in automation processes where an object is picked up from one location and transferred to another location.

We consider the simplest pick-and-place type task where the load is rotated from one position A to another position B, as shown in Fig. 2b. A feasible desired trajectory for such a task is given by

$$\theta_d(t) = \frac{\pi}{2}\cos(\omega t), \tag{6}$$

where $\omega$ is the angular frequency of the oscillatory motion.

### C. Torque and Energy

We will now compute the torque and the energy required to track the desired motion. The results will be used to understand the requirements to perform the same task with and without the magnetic spring.

According to the model presented in this section, the motor torque is given by:

$$\begin{aligned}\tau_m &= J\ddot{\theta}_d + b\dot{\theta}_d + k_s\theta_d \\ &= \frac{\pi}{2}(k_s - J\omega^2)\cos(\omega t) - \frac{\pi}{2}b\omega\sin(\omega t).\end{aligned} \tag{7}$$

Also, the input electrical power to the actuator can be calculated using the following relation:

$$p = IV = \frac{L}{2k_m^2}\frac{d}{dt}\tau_m^2 + \frac{R}{k_m^2}\tau_m^2 + \tau_m\dot{\theta}_d. \tag{8}$$

Finally, the electrical energy input is given by the time integral of the power. For one cycle of oscillation from A-B-A, this integral is:

$$E = \int_0^T p dt = \frac{\pi^3 R}{4k_m^2\omega}((k_s - J\omega^2)^2 + b^2\omega^2) + \frac{\pi^3 b\omega}{4}, \tag{9}$$

where $T$ denotes the period for the desired trajectory.

### D. Analytical Predictions

The analytical formulas in the previous subsection were derived assuming steady-state oscillations. They show that when the magnetic spring is not attached to the motor, $k_s = 0$, the motor is required to generate torque to both accelerate the load $\tau_m\dot{\theta}_d > 0$ but also to decelerate the load $\tau_m\dot{\theta}_d < 0$, in addition to compensate for the frictional losses. On the other hand, when the optimized magnetic spring, $k_s = J\omega^2$, is attached to the load, the magnetic spring provides the torque to both accelerate and decelerate the load, and the motor is only required to compensate for the

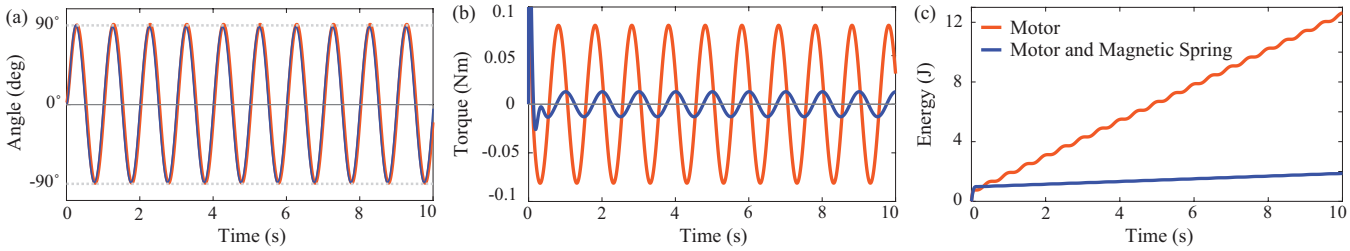


Fig. 3. Simulation results: (a) Desired trajectory. (b) Motor torque. (c) Electrical energy consumption. The figures show that despite following the same trajectory, the magnetic spring can significantly reduce the motor torque and the energy required to achieve the oscillatory motion compared to the motor alone. The model parameters used in the simulation are: $J = 1.29 \cdot 10^{-3}$ kgm$^2$, $b = 1.33 \cdot 10^{-3}$ kgm$^2/s$, $R = 1.4\ \Omega$, $L = 1.7$ mH, $k_m = 64 \cdot 10^{-3}$ Nm$/A$, $\omega = 2\pi$ rad$/s$.

frictional losses $\tau_m \dot{\theta}_d = b\dot{\theta}_d^2 \geq 0$. As a result, the ratio between the maximum motor torque and the energy required per oscillation cycle with and without the magnetic spring is given by

$$\frac{\max \tau_m|_{k_s=J\omega^2}}{\max \tau_m|_{k_s=0}} = \frac{b}{\sqrt{J^2\omega^2 + b^2}} \leq 1, \tag{10}$$

and

$$\frac{E|_{k_s=J\omega^2}}{E|_{k_s=0}} = \frac{b(k_m^2 + bR)}{b(k_m^2 + bR) + J^2R\omega^2} \leq 1. \tag{11}$$

Consequently, at least during steady-state oscillatory motion, the maximum torque and the energy required by the motor to drive the load is greater when not using the magnetic spring compared to when using the magnetic spring.

### E. Numerical Predictions

Figure 3 shows the trajectory, torque, and energy during the same pick-and-place task when the robot is controlled with the motor alone or the motor and the magnetic spring together in the arrangement shown in Fig. 2a. Despite the initial transient effect, we find that a larger maximal motor torque and more energy are required to perform the oscillatory task when using the motor alone compared to when using the motor with the magnetic spring. The numerical simulation results in Fig. 3 are consistent with the analytical predictions summarized in Section II-D.

## III. Optimization of a Magnetic Spring

In the previous section, we assumed that the magnetic spring is designed to have a linear torque-angle relation (3) as this relation was optimal for the linear model (1) and the sinusoidal desired motion (6). In general, however, the optimal torque-angle relation depends on the dynamics and the desired motion, and as such, it may not necessarily be linear. In what follows, we present an optimization framework to design the magnetic spring for arbitrarily complex dynamics and desired trajectory.

Our design method is detailed in Fig. 4; it consists of four steps: (a) setting the desired motion and the corresponding desired torque, (b) modeling a complex torque function of the magnetic spring with a sum of simple torque functions, (c) optimizing the simple torque functions to best approximate the desired torque function, and (d) arranging the permanent magnets according to the result of the optimization. In the remainder of this section, we will detail these four steps.

### A. Setting the Desired Motion and Torque

We assume that the desired motion and the desired torque are set (as shown in Fig. 4a,b), and given by:

$$\theta = \theta_d(t) \quad \text{and} \quad \tau = \tau_d(t). \tag{12}$$

The desired motion may be set without model-based computation, it could be a minimum jerk trajectory [18], or may be computed using model-based optimization [19]. Once the desired motion is set, the desired torque – torque required to implement the desired motion – can be computed using the model of the controlled system, as in Section II-C, or it may be measured as the output of a feedback controller used to track the desired trajectory, as in Section II-E).

### B. Model of the Magnetic Spring

A magnetic spring is an energetically passive device that cannot do net mechanical work on any closed path, for example, along the A-B-A path shown in Fig. 2b. However, a magnetic spring may be able to reproduce any energetically passive torque function, not limited to the linear function (3) used in Section II-A. Nevertheless, it is complicated to design a magnetic spring that can approximate a complex torque function which is energetically passive.

We proceed by approximating a complex torque function of the magnetic spring using a finite sum of simple torque functions:

$$\tau_s(\theta; a_i, \theta_i, \sigma_i) = \sum_{i=1}^{n} 2\frac{a_i}{\sigma_i}\left(\frac{\theta - \theta_i}{\sigma_i}\right) e^{-\left(\frac{\theta-\theta_i}{\sigma_i}\right)^2}, \tag{13}$$

where $a_i$ is the amplitude, $\theta_i$ is the center, and $\sigma_i$ is the width of the $i^{\text{th}}$ simple torque function. Each torque function can be obtained by taking the partial derivative of a potential energy function, and therefore, the sum of all these simple functions is energetically passive [20].

### C. Minimizing the Active Torque of the Motor

The next step is to minimize the difference between the desired torque $\tau_d$ and the torque provided by the magnetic spring $\tau_s$ along the desired trajectory. This minimization is

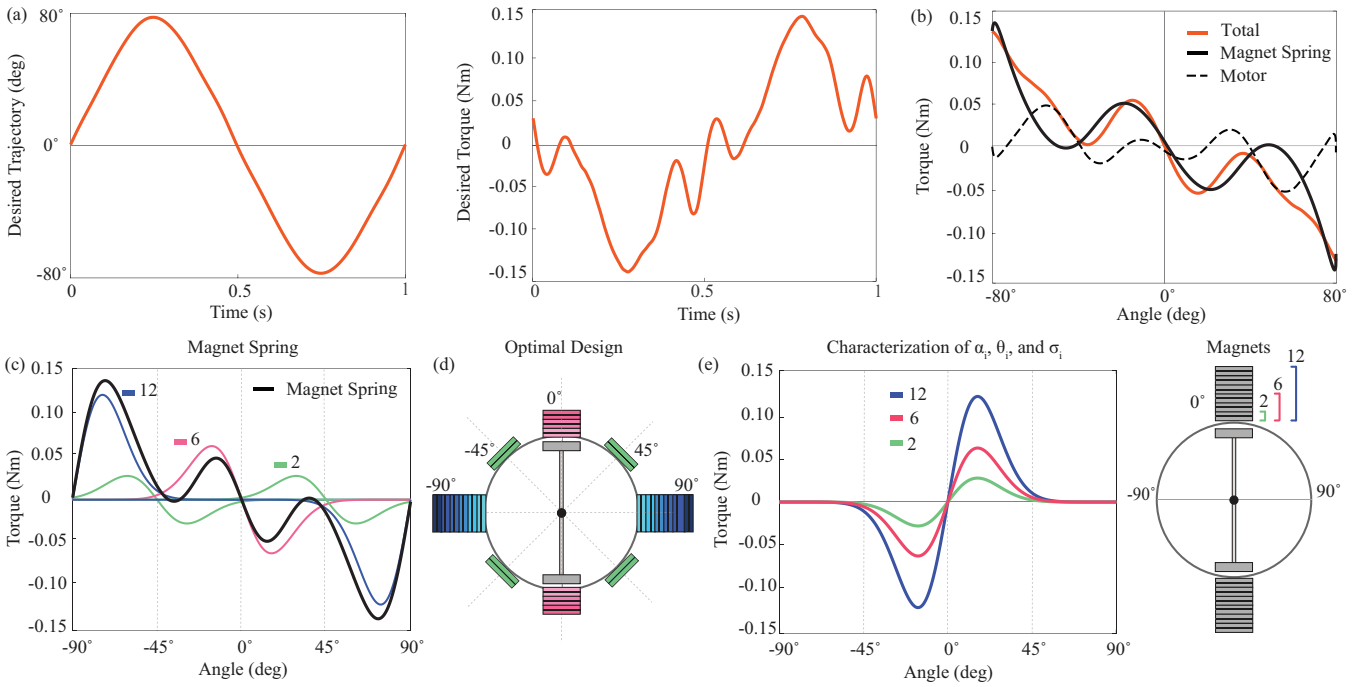


Fig. 4. Design method: (a) Desired trajectory and desired torque. (b) Complex torque function of the magnetic spring as a sum of motor torque and spring torque. (c) Optimal magnetic spring torque function. (d) Arrangement of permanent magnets according to the optimization. (e) Experimental local torque deflection characteristic of a magnet dipole.

equivalent to minimizing the active torque $\tau_m$ that must be provided by the motor:

$$\min_{a_i,\theta_i,\sigma_i} \int_0^T || \underbrace{\tau_d(t) - \tau_s(\theta_d(t); a_i, \theta_i, \sigma_i)}_{\approx \tau_m} ||^2 dt \qquad (14)$$

$$\text{subject to} \quad a_i \in [a_{i\,\min}, a_{i\,\max}],\ \theta_i \in [0, 2\pi], \sigma_i \geq 0.$$

The solution of this optimization problem defines the complex passive torque-angle function for the optimal magnetic spring (13), as shown in Fig. 4b (solid black line), and the additional active torque that must be provided by the motor, as shown in Fig. 4b (dashed black line).

The optimal solution also provides the decomposition of the complex torque function of the magnetic spring to multiple simple torque functions (13), as shown in Fig. 4c, and defines the free parameters of the simple torque functions, namely, $a_i$, $\theta_i$, and $\sigma_i$ for $i \in \{1, 2, ..., n\}$. These parameters were used to design of the magnetic spring shown in Fig. 4d.

### D. Design of the Magnetic Spring

To establish the relation between the location, height, and width of the magnets, and the model parameters, $a_i$, $\theta_i$, $\sigma_i$, we have performed a simple characterization experiment. The results of the experiment are summarized in Fig. 4e.

Based on the values $a_i$, $\theta_i$, $\sigma_i$ computed using (14), and using the relations in Fig. 4e, we design the optimal magnetic spring shown in Fig. 4d. The benefit of using the magnetic spring is clearly shown in Fig. 4b. The figure shows that using the magnetic spring can significantly reduce the motor torque (dashed black line) compared to not using the magnetic spring (solid orange line).

The design procedure outlined in this section will be agnostic to the details of the robot dynamics and the complexity of the desired motion if the desired torque $\tau_d$ in (14) is the measured torque (instead of the model-based predicted torque) to move the robot along the desired trajectory. In Section IV, we present two actuator designs which are agnostic to the details of the dynamics and the desired motion.

## IV. Experimental Evaluation

In this section, we present the prototype of the magnetic spring actuator designed in Section III and presented in Fig. 4d. In addition, we show how to customize the actuator for a significantly different desired trajectory.

### A. Prototype

The prototype is composed of a motor coupled to the magnetic spring as shown in Fig. 5a. The magnetic spring is similar to a standard permanent magnet motor as it is composed of a rotor and a stator. The rotor has two magnets, one on each side, and is connected to the motor, shown in Fig. 5b,c (green parts). The surrounding cylindrical stator consists of sixteen possible magnet locations to stack from one to twelve magnets. The stack of magnets in one location represents one simple torque function, while all the magnets represent the total non-uniform torque angle function, mathematically represented by (13). The symmetric and asymmetric magnet arrangements in Fig. 5b,c correspond

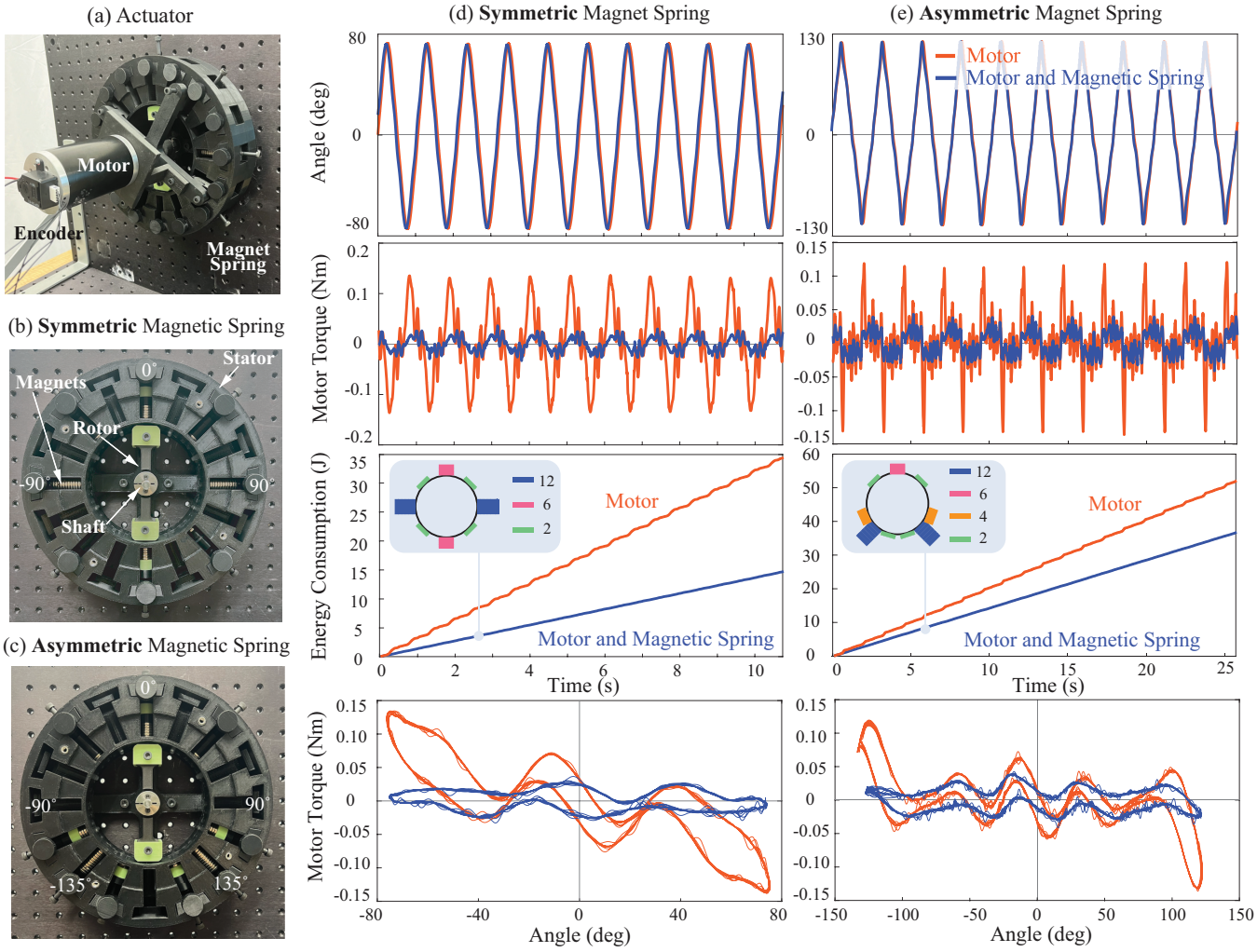


Fig. 5. Prototype and experimental data. (a) Actuator. (b) Symmetric magnetic spring design. (c) Asymmetric magnetic spring design. (d,e) Position, torque, energy, magnet configuration, and torque-angle relation of the magnetic springs. The results with the motor alone are shown with red lines. The results with the motor and the magnet spring are shown with blue lines.

to two different desired trajectories, one with $\pm 80^o$ and the other with $\pm 130^o$ amplitudes, as shown in Fig. 5d,e.

### B. Experimental Setup and Protocol

A Crouzet 89830912 DC motor was used for the experiment, with a Maxon ESCON 50/5 motor controller driving the motor in current control mode. The motor position, $\theta$, was measured using a Broadcom HEDM-5500 incremental encoder, and in-line motor current readings were obtained through the ESCON 50/5 motor driver. An INA219 current sensor was used to measure the motor power. Finally, a Teensy 4.1 microcontroller was used to read the encoder measurements, command the motor driver, obtain the current and power readings, and log the experimental data.

We used a proportional differential controller, with proportional $k_p$ and differential $k_d$ gains, to track the desired motion of the load,

$$\tau_d(t) = -k_p(\theta - \theta_d(t)) - k_d(\dot{\theta} - \dot{\theta}_d(t)).$$

We measured the rotation angle $\theta$ and the motor current $I$ when the motor was used alone and when the motor was used together with the magnetic spring. In both cases, we calculated the motor torque $\tau_m = k_m I$, using the measured motor current. Finally, we integrated the power measurement from INA219 over time to obtain the energy required by the motor $E$ to oscillate the load.

### C. Experimental Results

Figure 5 summarizes the experimental results. In the first experiment, the load oscillated with $\pm 80^o$ amplitude along a non-sinusoidal trajectory using a motor and a symmetric magnetic spring design shown in Fig. 5b. We observed over $50\%$ reduction in both the peak torque and the energy cost per oscillation cycle when the magnetic spring was utilized compared to the motor alone, see Fig. 5d.

In order to demonstrate customization of the actuator by rearrangement of the magnets, we repeated the procedure in Section III to redesign the magnetic spring for a different

desired non-sinusoidal trajectory with $\pm 130^o$ amplitude. The new actuator has a non-symmetric magnetic spring design shown in Fig. 5c. Using this actuator, we observed somewhat smaller but still notable torque reduction and energy saving as shown in Fig. 5e. The reduction of the motor torque and energy during steady-state operation is attributed to the effect of the optimized magnetic spring since the trajectories with and without the magnetic spring were nearly identical as shown in Fig. 5d,e.

These results not only highlight the ease of customization of the proposed magnetic spring actuator but also corroborate our theoretical predictions from Section II, demonstrating that using a motor with a task-optimized non-uniform permanent magnetic field can provide substantial energy saving compared to using a motor alone for oscillatory tasks.

## V. Discussion and Conclusion

In this paper, we introduced a novel magnetic spring actuator and demonstrated its effectiveness in reducing energy consumption for oscillatory tasks compared to direct-drive motors. Whereas previous works mainly focused on improving the mechanical design and characterization of magnetic springs [15], [16], here we focused on optimizing magnetic spring designs to create customizable actuators that can effectively reduce energy consumption in various oscillatory tasks.

The proposed magnetic spring actuator generalizes permanent magnet motors by allowing a systematic design optimization of the actuator for repetitive tasks. By strategically arranging permanent magnets, we can achieve desired magnetic spring characteristics, resulting in substantial motor torque reduction and energy savings, in addition to a significant reduction of the proportional and differential control gains required to track the same desired trajectory.

We employed two significantly different desired trajectories to demonstrate the ease of customization of the magnetic spring actuator. Customization allows our magnetic spring actuator to be easily tailored for diverse oscillatory tasks while maintaining high efficiency. This adaptability underscores the actuator's potential to effectively meet specific task requirements.

In future work, we aim to enhance the proposed actuator concept by adding the capability to dynamically adjust the magnetic potential field during motion, potentially using electromagnets [21] or other mechanisms [22]. We aim to design a compact actuator with adaptable optimal torque-deflection characteristics for various tasks, including fast oscillatory pick and place tasks and locomotion tasks, in addition to exploring the concept of an optimal actuator that seamlessly adapts its torque-deflection characteristic between different desired motions and tasks in real-time.

## References


[1] S. Wang, W. van Dijk, and H. van der Kooij, "Spring uses in exoskeleton actuation design," in *IEEE International Conference on Rehabilitation Robotics*, pp. 1–6, 2011.

[2] D. F. B. Haeufle, M. D. Taylor, S. Schmitt, and H. Geyer, "A clutched parallel elastic actuator concept: Towards energy efficient powered legs in prosthetics and robotics," in *IEEE RAS & EMBS International Conference on Biomedical Robotics and Biomechatronics*, pp. 1614–1619, 2012.

[3] M. Plooij, M. Wisse, and H. Vallery, "Reducing the energy consumption of robots using the bidirectional clutched parallel elastic actuator," *IEEE Transactions on Robotics*, vol. 32, no. 6, pp. 1512–1523, 2016.

[4] A. Mazumdar, S. J. Spencer, C. Hobart, J. Salton, M. Quigley, T. Wu, S. Bertrand, J. Pratt, and S. P. Buerger, "Parallel elastic elements improve energy efficiency on the steppr bipedal walking robot," *IEEE/ASME Transactions on Mechatronics*, vol. 22, no. 2, pp. 898–908, 2017.

[5] B. M. Wisse, W. D. van Dorsser, R. Barents, and J. L. Herder, "Energy-free adjustment of gravity equilibrators using the virtual spring concept," in *IEEE International Conference on Rehabilitation Robotics*, pp. 742–750, 2007.

[6] S. H. Collins, M. B. Wiggin, and G. S. Sawicki, "Reducing the energy cost of human walking using an unpowered exoskeleton," *Nature*, vol. 522, pp. 212–215, 6 2015.

[7] Y. Li, Z. Li, B. Penzlin, Z. Tang, Y. Liu, X. Guan, L. Ji, and S. Leonhardt, "Design of the clutched variable parallel elastic actuator (CVPEA) for lower limb exoskeletons," in *Annual International Conference of the IEEE Engineering in Medicine and Biology Society (EMBC)*, pp. 4436–4439, 2019.

[8] T. Wang, T. Zheng, S. Zhao, D. Sui, J. Zhao, and Y. Zhu, "Design and control of a series–parallel elastic actuator for a weight-bearing exoskeleton robot," *Sensors*, vol. 22, p. 1055, 1 2022.

[9] C. W. Mathews and D. J. Braun, "Parallel variable stiffness actuators," in *IEEE/RSJ International Conference on Intelligent Robots and Systems*, pp. 8225–8231, 2021.

[10] C. W. Mathews and D. J. Braun, "Design of parallel variable stiffness actuators," *IEEE Transactions on Robotics*, vol. 39, no. 1, pp. 768–782, 2023.

[11] W. Robertson, B. Cazzolato, and A. Zander, "A multipole array magnetic spring," *IEEE Transactions on Magnetics*, vol. 41, no. 10, pp. 3826–3828, 2005.

[12] C. Forbrigger, A. Schonewille, and E. Diller, "Tailored magnetic torsion springs for miniature magnetic robots," in *IEEE International Conference on Robotics and Automation*, pp. 7182–7188, 2021.

[13] F. Poltschak and P. Ebetshuber, "Design of integrated magnetic springs for linear oscillatory actuators," in *XXII International Conference on Electrical Machines (ICEM)*, pp. 729–735, 2016.

[14] J. Chen, Z. Liang, Y. Zhu, C. Liu, L. Zhang, L. Hao, and J. Zhao, "Towards the exploitation of physical compliance in segmented and electrically actuated robotic legs: A review focused on elastic mechanisms," *Sensors*, vol. 19, no. 24, 2019.

[15] B. Kozakiewicz and T. Winiarski, "Spring based on flat permanet magnets: Design, analysis and use in variable stiffness actuator," *Facta Universitatis, Series: Mechanical Engineering*, vol. 21, no. 1, pp. 101–120, 2023.

[16] A. Sudano, D. Accoto, L. Zollo, and E. Guglielmelli, "Design, development and scaling analysis of a variable stiffness magnetic torsion spring," *International Journal of Advanced Robotic Systems*, vol. 10, pp. 1–11, 01 2013.

[17] N. Gori, C. Simonelli, A. Musolino, R. Rizzo, E. Díez Jiménez, and L. Sani, "Design and optimization of a permanent magnet-based spring–damper system," *Actuators*, vol. 12, no. 7, 2023.

[18] T. Flash and N. Hogan, "The coordination of arm movements: an experimentally confirmed mathematical model," *Journal of Neuroscience*, vol. 5, no. 7, pp. 1688–1703, 1985.

[19] D. J. Braun, F. Petit, F. Huber, S. Haddadin, P. van der Smagt, A. Albu-Schaffer, and S. Vijayakumar, "Robots driven by compliant actuators: Optimal control under actuation constraints," *IEEE Transactions on Robotics*, vol. 29, no. 5, pp. 1085–1101, 2013.

[20] A. Sutrisno, "Analitical design of energetically passive mechanisms," Master's Thesis, Vanderbilt University, Nov 2023.

[21] M. Li, Q. Xiao, Z. Wang, C. Liu, and K. Bai, "A variable stiffness spherical joint motor by magnetic energy shaping," *IEEE Transactions on Robotics*, vol. 40, pp. 1410–1420, 2024.

[22] A. Sudano, N. L. Tagliamonte, D. Accoto, and E. Guglielmelli, "A resonant parallel elastic actuator for biorobotic applications," in *IEEE/RSJ International Conference on Intelligent Robots and Systems*, pp. 2815–2820, 2014.